Energy

FOSSIL

DOE/PC/50052-T1
(DE84009755)

MODELING OF CWM DROPLET COMBUSTION

Final Report

By
Krish Pandalai
Suresh Aggarwal
William Sirignano

October 1983

Work Performed Under Contract No. AC22-82PC50052

Pandalai Coatings Company
Brackenridge, Pennsylvania

Technical Information Center
Office of Scientific and Technical Information
United States Department of Energy

DISCLAIMER

DISCLAIMER

This report has been reproduced directly from the best available copy.

Available from the National Technical Information Service, U. S. Department of Commerce, Springfield, Virginia 22161.

Price: Printed Copy A03
Microfiche A01

Codes are used for pricing all publications. The code is determined by the number of pages in the publication. Information pertaining to the pricing codes can be found in the current issues of the following publications, which are generally available in most libraries: *Energy Research Abstracts (ERA); Government Reports Announcements* and Index (*GRA* and I); *Scientific and Technical Abstract Reports (STAR);* and publication NTIS-PR-360 available from NTIS at the above address.

DOE/PC/50052-T1
(DE84009755)
Distribution Category UC-90b

Modeling of CWM Droplet Combustion

Krish Pandalai, Pandalai Coatings Company
Suresh Aggarwal, Carnegie - Mellon University
William Sirignano, Carnegie - Mellon University

Prepared For

Department of Energy
Pittsburgh Energy Technology Center
Pittsburgh, PA.

Contract No: DE-AC22-82PC50052

October 1983

PANDALAI COATINGS COMPANY
Brackenridge, PA.

Abstract

The objective of the present study was to develop a one-dimensional, unsteady state model for coal-water mixture droplet combustion, and to compare the characteristic times for the various processes, such as water vaporization, devolatilization and char oxidation with available experimental data.

A water film surrounding a spherical coal particle is considered to undergo vaporization by heat transfer from the hot air. After the water vaporization is complete, devolatilization begins. This process is assumed to be kinetically controlled. Water vaporization and devolatilization processes are modeled by using a hybrid Eulerian-Lagrangian method to obtain the properties of the gas-phase and the condensed-phase. An explicit finite difference scheme is used to solve the Eulerian gas-phase equation where as a Runga-Kutta scheme is employed to solve the Lagrangian condensed-phase equations. The predicted characteristic times for water vaporization is in good agreement with values proposed in the literature. At the present time there is insufficient data to draw any conclusions on the model. Methods are proposed to refine the simple kinetic model which takes into account pore diffusion and mass transfer for devolatilization and char oxidation.

TABLE OF CONTENTS

1. Introduction

Considerable interest in coal-water mixture combustion has been generated in the recent past due to the efforts of the fossil fuel and combustion division of the Department of Energy. It has been demonstrated that a stable coal-water mixture containing about 60-70% solids loading can be made, atomized and burnt in a conventional industrial boiler. In order to design a boiler with maximum efficiency, it is essential that a theoretical basis be developed to predict combustion kinetics. It is important to know whether the kinetics or the mixing phenomenon determines the rate controlling step in the overall combustion process. Depending upon the type of coal, the composition and porosity varies a great deal.

For the proper design of a combustor, using Coal-Water Mixture (CWM) fuel, a knowledge of the characteristic times for the various combustion processes (water vaporization, devolatilization, and char oxidation) is necessary. A model to predict these variables accurately is lacking at the present time.

Solomon and Colket (1) obtained devolatilization data over a wide range of experimental conditions and for a variety of coals. These researchers report good agreement between theory and experiment using a single set of rate parameters which vary with volatile species, but are independent of coal type. The activation energies and Arrhenius pre-exponential factors appear to be lower than that obtained by other

investigators. Solomon and Colket (1) consider only kinetic parameters, pore diffusion and mass transfer contributions are neglected in the above study. Work done by Suuberg, Peters, and Howard (2) indicate that lignite volatiles are dominated by CO, CO_2, and H_2O while volatiles from the bituminous coal are tar and light hydrocarbons. The kinetics of lignite devolatilization was modeled by one, two, or three first-order decomposition reactions. For the devolatilization modeling of bituminous coal, evaporation and diffusion of tar along with pyrolytic and secondary reactions have been considered. Smoot (3) has given an excellent review article on pulverized coal diffusion flame. Modeling efforts of various researchers are summarized in the review article. The characteristic times for devolatilization is around 10-100 milliseconds whereas the char oxidation time is of the order of one minute. Clearly the rate controlling step is the char oxidation step. Even though devolatilization step is ten times faster than char oxidation, the stability of a CWM flame is attributed to the high volatiles present in CWM. Therefore devolatilization is very important in the combustion of a fuel such as CWM. Since char is the product obtained after devolatilization, the rate amount and type of volatiles evolved all have a bearing on the structure of the char formed. Some of the chains are presumed to be broken and then repolymerized during devolatilization. Unger and Suuberg (4) developed a model which considers mass transfer in and around pyrolyzing coal particles. The agreement between theory and experiment is pretty good at one atmosphere pressure, but off by an order of magnitude of two at different pressures.

The first step in the overall combustion process is water vaporization. The model developed in the present study considers rates of water vaporization, water temperature and coal particle temperature prior to completion of vaporization. The second step is the devola tilization. Some breakdown of the aromatic ring compounds in coal take place and these gases escape during devolatilization. For proper flame stability the presence of these volatiles is very important as pointed out earlier. There is some evidence to show that repolymerization also takes place. Char oxidation is the third step and the characteristic times reported for this step is of the order one second compared to 50-100 milliseconds for vaporization and devolatilization steps. Depending upon the particle size, diffusion rate or surface reaction rate could control the char oxidation step. If the diffusion rate is sufficiently low and/or if the surface oxidation rate is sufficiently high (large particles and/or high particle temperature), the reaction would primarily occur at the outer char surface. For larger film diffusion rates, a significant amount of diffusion into the pores occur with heterogeneous oxidation and internal heterogeneous oxidation.

The objective of this research is to develop a sound theoretical model to predict the characteristic times and the rate of combustion of coal-water mixture (CWM). This information is necessary for the proper design of a furnace using CWM as the fuel. Equations of continuity, energy and momentum would be developed for the two cases, i.e., individual droplet and slurry.

The equations that govern the behavior of the burning of coal-water slurries are a challenging system. The subsystem of equations governing the gas-phase properties have elliptical spatial operators while the subsystem governing the droplet and particle properties will be hyperbolic. Generally a hybrid numerical scheme is desirable with an Eulerian finite-difference scheme for the gas-phase and a Lagrangian finite-difference scheme for the condensed-phase properties, i.e., internal process of water vaporization, devolatilization and char oxidation are better followed by employing a Lagrangian scheme. Following this approach a numerical study been conducted to predict the particle heating, water vaporization and devolatilization processes for a coflowing air and coal-water slurry spray. The char oxidation process is not examined in the present case. The physical model and the governing equations for the two phases are discussed in section 2. The results are presented in section 3. A method to include the pore diffusion in the devolatilization and char oxidation processes is discussed in the Appendix.

2. A Spray Model for Water Vaporization and Devolatilization

2a. Physical Model

This section gives the details of a spray model, shown schematically in Figure 1 for describing the laminar one-dimensional transient flow of air and coal-water-slurry droplets in an open tube. Conditions at the tube entrance are prescribed. Air flow is continuous, whereas the droplets are injected intermittently. The frequency of injection is determined by

prescribing the mass flow rate of the condensed phase, the number of droplets per unit area of the tube, the initial droplet size, and density. A dilute monodisperse spray without any droplet interaction is considered.

Droplet dynamics, droplet heating, water vaporization, and devolatilization processes are considered in the present study. The dynamics is modeled by using a drag law, where the drag coefficient is a function of the Reynolds number based on the relative velocity of the droplet with respect to gas the the droplet radius. The functional form of the drag coefficient is the same as used in Ref. (5). The droplet heating is modeled by assuming that the droplet temperature is spatially uniform but temporally varying. Water vaporization and devolatilization processes are assumed to be mutually exclusive events. In modeling of these processes, it is further assumed that the water surrounds the coal particle (see Fig. 1). Following its introduction into the hot air flow, a droplet first gets heated, without appreciable water vaporization, to its wet-bulb temperature. This is followed by a period of water vaporization, during which the droplet temperature remains almost constant. After the water vaporization is completed. droplet heating and devolatilization processes follow. In addition, the droplets continuously accelerate since initially a higher velocity is provided for the gas phases. The above condensed-phase processes influence the state of the gas, i.e., the gas-phase is continuously retarded, cooled, and enriched with water vapor and volatiles. All these gas-phase and condensed processes are modeled by a system of unsteady, one-dimensional equations. The gas-phase is represented in Eulerian coordinates and the liquid-phase is represented in Lagrangian coordinates. The governing equations in the non-dimensional form are given as follows:

2b. Gas-Phase Equations

$$\frac{\partial \rho}{\partial t} + \frac{\partial}{\partial x}(\rho v) = S_{\rho} \tag{1}$$

$$\frac{\partial Y}{\partial t} + v\frac{\partial Y}{\partial x} - \frac{t_l}{\rho}\frac{\partial}{\partial x}\left(\rho D \frac{\partial Y}{\partial x}\right) = S \tag{2}$$

where

$$Y = Y_w, Y_v, Y_o, \Phi \tag{3}$$

$$S = S_w, S_v, S_o, S_{\Phi} \tag{4}$$

$$Y_n = 1 - Y_w - Y_v - Y_o \tag{5}$$

$$\Phi = T\, p^{\Gamma}, \qquad \Gamma = \frac{1-\gamma}{\gamma} \tag{6}$$

$$\rho = \frac{p^{1/\gamma}}{\Phi} \tag{7}$$

2c. Condensed-Phase Equations

$$\frac{d X_k}{dt} = V_k \tag{8}$$

$$\frac{d V_k}{dt} = \left\{ \rho_r \, t_r \, L_r^2 \right\} \frac{3}{16} \frac{C_D \, \rho \, D}{\rho_k \, r_k^2} \, R_{ek} \, (V - V_k) \tag{9}$$

$$\frac{d r_k^2}{dt} = - \left\{ \rho_r \, t_r \, L_r^2 \right\} \frac{2 \, \rho \, D}{\rho_k} \, m_{wk} \tag{10}$$

$$\frac{d T_k}{dt} = F_1 \, I_w + (1 - I_w) \, F_2 \tag{11}$$

$$F_1 = 3 \left\{ \rho_r \, t_r \, L_r^2 \right\} \frac{\rho \, D \, m_{wk} \, (H_k - L_w)}{C_{pk} \, \rho_k \, r_k^2} \tag{12}$$

$$F_2 = 3 \left\{ \rho_r \, t_r \, L_r^2 \right\} \frac{R_f \, \rho \, D \, C_p \, (T - T_k)}{C_{pk} \, \rho_k \, r_k^2} \tag{13}$$

$$\rho_k = \rho_c \left(\frac{r_c}{r_k} \right)^3 + \rho_w \left[1 - \left(\frac{r_c}{r_k} \right)^3 \right] \tag{14}$$

$$\rho_k \, C_{pk} = C_{pc} \, \rho_c \left(\frac{r_c}{r_k} \right)^3 + C_{pw} \, \rho_w \left[1 - \left(\frac{r_c}{r_k} \right)^3 \right] \tag{15}$$

$$\frac{d m_{rk}}{dt} = - m_{rk} \sum_{m=1}^{M} K_m \tag{16}$$

$$\frac{d\, m_{chk}}{dt} = m_{rk} \sum_{m=1}^{M} K_m (1-\alpha_m) \tag{17}$$

$$m_k = m_{rk} + m_{chk} + m_{ak} \tag{18}$$

$$\rho_k = \frac{3\, m_k}{4\pi\, r_k^3} \tag{19}$$

$$C_D = \frac{24}{R_{ek}} \left(1 + \frac{R_{ek}^{2/3}}{6}\right) \tag{20}$$

$$R_{ek} = \frac{2}{t_r\, L_r} \frac{r_k\, \rho}{\mu} \left| V - V_k \right| \tag{21}$$

$$\mu' = \mu' (T_r') = \frac{1.458 \times 10^{-5}\, T_r'^{3/2}}{110.4 + T_r'} \tag{22}$$

$$\text{where} \quad T_r' = \frac{1}{3} T' + \frac{2}{3} T_k' \tag{23}$$

2d. Source Terms for the Gas Phase

$$S_\rho = \sum_k \frac{n_k}{\Delta x} \left[\frac{t_r}{L_r} M_{wk} + M_{vk}\right] \tag{24}$$

$$S_w = \frac{1}{\rho} \sum \frac{n_k}{\Delta x} \left[\frac{t_r}{L_r} M_{wk} (1-Y_w) - Y_w M_{vk} \right] \quad (25)$$

$$S_v = \frac{1}{\rho} \sum \frac{n_k}{\Delta x} \left[- \frac{t_r}{L_r} M_{wk} Y_v + M_{vk} (1-Y_v) \right] \quad (26)$$

$$S_o = - \frac{Y_o}{\rho} S_\rho \quad (27)$$

$$S_\Phi = - \frac{p\Gamma}{\rho} \sum \frac{n_k}{\Delta x} \left[\frac{t_r}{L_r} M_{wk} \left\{ H_k + C_p (T-T_k) \right\} \right.$$

$$\left. + Q_k \frac{t_r}{L_r} + M_{vk} C_p (T-T_k) \right] \quad (28)$$

where

$$M_{wk} = 4\pi \rho D r_k m_{wk} \quad (29)$$

$$m_{wk} = I_w R_f \ell n (1 - B_k \quad (30)$$

$$B_k = \frac{Y_{ws} - Y_k}{1-Y_{ws}} = \frac{C_p (T-T_k)}{H_k} \quad (31)$$

$$R_f = 1 + 0.3 R_{ek}^{.5} \quad (32)$$

$$H_k = (1 - Y_{ws}) C_p (T - T_k)/(Y_{ws} - Y_w) \quad (33)$$

$$Y_{ws}^{-1} = 1 + \frac{M_a'}{M_w'} \left(X_{ws}^{-1} - 1 \right) \tag{34}$$

$$X_{ws} = \frac{p_n'}{p'} \exp \left[\frac{L_w' M_w'}{R'} \left(\frac{1}{T_{bn}'} - \frac{1}{T_k'} \right) \right] \tag{35}$$

$$I_w = 1 \quad \text{during water vaporization}$$

$$= 0 \quad \text{after water vaporization} \tag{36}$$

$$M_{vk} = \frac{(1 - I_w)}{\rho_r L_r^3} \sum_{m=1}^{M} K_m \alpha_m m_{rk}', \quad M = 2 \tag{37}$$

$$K_m = A_m \, \text{Exp} \left(- T_m / T_k \right), \quad m = 1,2 \tag{38}$$

$$Q_k = 4\pi R_f r_k \rho D C_p (T - T_k) \tag{39}$$

Note that a transformed temperature as given by Eq. (6), has been employed. This transformation, which is useful for constant volume situation, has been retained here (a constant pressure case) for the sake of generality. Also, the inclusion of oxidizer species in the gas-phase, though redundant for the calculations reported here, is for the sake of generality. Of course, this will be required for the char oxidation study.

For non-dimensionalizing the gas-phase equations, the tube length and the gas velocity at the tube entrance are used as the length scale and the velocity scale respectively. The time scale is determined by these two scales. The gas-phase properties are non-dimensionalized by using the

respective properties at the entrance. For the condensed phase, the droplet position, velocity and temperature are respectively non-dimensionalized by the gas-phase length, velocity and temperature scales. The droplet radius and density are non-dimensionalized by the initial droplet radius and the coal density respectively. The above non-dimensionalization gives rise to three additional dimensionless groups t_r, L_r and ρ_r ; t_r is the ratio of convective time to diffusion time in the gas-phase, L_r is the ratio of gas-phase length scale and the initial drop radius, and ρ_r is the ratio of initial gas-phase density and the condensed-phase density.

The important assumptions made in writing the gas-phase equations are that the gas pressure is constant, the radiative heat transfer is negligible, the species diffusion follows Fick's law with equal mass diffusivities for each paper, the specific heats are constant and equal and the gas-phase Lewis and Schmidt numbers are constant. In addition, the product ρD is assumed constant. It is noteworthy, however, that for the calculation of condensed-phase Reynolds number (Eq. 21), μ is considered a function of temperature (see Ref. 5) as given by Eqs. (22) and (23).

For the condensed-phase equations, the important assumptions and the various features are discussed below:

1. The effect of gas-phase convection on the water vaporization and particle heating is given by a Ranz-Marshall correlation [6] as indicated in Eq. (30).

2. The water-vaporization process is diffusion-controlled, where the diffusion rate is mainly determined by the water vapor mass fraction at the droplet surface and that in the gas environment. A phase equilibrium relation (Clasius-Clapeyron relation as given by Eq. (35)) is used to calculate the water vapor mass fraction at the surface.

3. During the waver-vaporization period, the particle density is given by Eq. (25). These values are required in relation (11).

4. After water vaporization is completed, the particle temperature starts rising again. The heat transfer rate from the gas-phase to the particle is based on a Nusselt number for a solid sphere with a convective correction as given by Ranz-Marshall correlation.

5. As the particle temperature rises, the devolatilization process is initiated. The devolatilization is assumed to be kinetically controlled and the effect of pores is neglected in the present calculations. The rate of devolatilization is assumed to be given by two competing first-order reactions as discussed by Ubhayakar et al. [7]. A single first-order reaction scheme is found to be inadequate to explain the measured volatile yields over a range of conditions [8]. Since the amount and rate of measured volatile yields is much higher at higher temperatures, the two reaction scheme of Ref. [7] and that of Ref. [8] gives a much better fit to the experimental data. Note that both the references have used similar reaction schemes but with different values of the reaction rate parameters. In the present study the parameter values are taken from Ref. [7]. These values have also been used by Smith and Smoot [9].

The initial conditions, boundary conditions, and the solution procedure are the same as those used in Ref. [5]. Essentially an hybrid Eulerian-Lagrangian method has been used to solve the two-phase equations. An explicit finite-difference scheme is used to solve the Eulerian gas-phase equations whereas a second-order Runge-Kutta scheme is employed to solve the Lagrangian condensed-phase equations.

3. Results

Results for particle heating, water vaporization, and devolatilization processes are shown in Figs. 2-12. A mixture of air and monodisperse spray of coal-water slurry flowing in a tube is considered. Values of all the parameters used in the calculations are listed in Table 1. Initially each particle is composed of 50 percent of coal and 50 percent of water by volume. For a coal specific gravity of 1.5, this amounts to 60 percent coal by weight in each particle. The initial coal composition is assumed to be 90 percent raw coal, 5 percent char and 5 percent ash. During devolatilization process, raw coal yields char and volatiles. The air flow is continuous, whereas the slurry flow is intermittent. The frequency of injection is determined after prescribing the mass flow rate of the slurry, particle radius, and the number of particles per unit area (or number of particles in a group). For the present calculations one group (of particles) is injected after every 25 msec and there are 400 particles in each group. This amounts to a slurry flow rate of 0.104 gram per second per unit area, whereas the corresponding air flow is 0.47.

Figure 2 gives the particle position in the tube versus time for different particle groups. Only a few representative groups are shown. For example, between group '1' and group '5' there are four additional particle groups. The instant of injection, given by the time at position x_k=o, identifies the different particle groups. As Fig. 2 indicates, the residence time for a particle is about 64 msec. The variation of velocity with time for different particle groups is given in Fig. 3. The initial particle velocity is 20 cm/sec, whereas the gas velocity is 200 cm/sec at the tube entrance. The particles accelerate at a decreasing rate which approaches nearly zero after 20 msec. Note that for groups '10', '20', and '30', the starting point for the velocity plot does not appear to be at 20 cm/sec. This is due to the difference in the actual injection instant and the instant plotting is starting. For example, group '10' is injected at 22.5 msec, whereas the plotting is started at 23 msec. The particle size variation with time is given in Fig. 4. The particle heating period, when the water vaporization rate is negligible, is about 2.0 msec. Then the particle size decreases continuously until the water vaporization is completed. The time for complete water vaporization is about 25 msec, after which the devolatilization starts and the particle size remains constant. As Fig. 5 shows, it takes about 3.0 msec for the particle temperature to attain its wet-bulb value. At the wet-bulb temperature, the heat supplied from the gas phase goes as the latent heat of vaporization without raising particle temperature. Thus the temperature remains almost constant until the water vaporization is complete. Then it starts increasing again during the devolatilization period. The particle temperature reaches a value of about 1140°K at the tube exit. The particle density plots are

given in Fig. 6. During the water vaporization period, the particle density is the average of coal density and water density. Consequently as the water vaporizes, the particle density increases. When the water vaporization is complete, the density starts decreasing due to devolatilization. Note that the particle radius is assumed constant during the devolatilization process.

The history of devolatilization process is shown in Figs. 7-8. The variation of raw coal mass fraction in the coal particle with time is given in Fig. 7. Initially this mass fraction is 0.9. When the devolatilization starts (after 30 msec), raw coal yields char and volatiles. As a result, its mass fraction decreases continuously. Since the particle temperature is increasing, the rate of decrease of raw coal mass fraction increases. The increase of char mass fraction with time is demonstrated in Fig. 8. Initially its value is 0.05 and it increases at an increasing rate. Note that for particle group '1' the char mass fraction seems to become constant after 65 msec. This is simply due to the fact that this group has reached the tube exit at this time. (see Fig. 2)

The profiles of gas-phase properties in tube at different instances of time are shown in Figs. 9-12. The profiles given in Fig. 9 indicate that the gas temperature continuously decreases due to the heat transfer to the condensed phase. Note that the oscillations in the gas temperatures are well-behaved and are entirely due to the periodic nature of the particle injection process which causes a finite droplet spacing in the streamwise direction. Also note that the period of this oscillation is the same as the

time interval between two subsequent injections. These oscillations are observed in the other gas-phase properties. The profiles of water vapor mass fraction are given in Fig. 10. The water vaporization is completed at about 25 msec (the corresponding axial location is 3.5 cm), after which the profiles change mainly due to the gas-phase convection. The volatile mass fraction profiles, shown in Fig. 11, indicate that the devolatilization starts at about 25 msec (after the water vaporization is completed). Note that the devolatilization starts becoming significant only after 35 msec (see also Fig. 7). It is also worth noting that the devolatilization process is not complete in the present calculations. A larger residence time is required for its completion. Figure 12 gives the gas velocity plots. The gas velocity continuously decreases due to the momentum transfer to the condensed-phase. Note that for time = 10 msec (also 40 msec) the gas velocity profiles should finally recover the value 200 cm/sec at some point in the tube. That is not the case in the present calculations because pressure is assumed uniform.

Conclusions

It has been shown that the unsteady state one-dimensional model developed in the present work adequately predicts the initial water vaporization rate in the coal-water mixtures combustion process. Condensed-phase and gas-phase properties could be calculated from the model and the characteristic time for water vaporization calculated has been found to be in agreement with values reported in the literature. A

beginning in the modeling of the devolatilization process has been made in the present study. A two-step chemical kinetic reaction scheme has been used to develop the model. More work is necessary to calculate the characteristic time required for complete devolitization and char oxidation. This model willl includue pore-diffusion and mass-transfer. The basic equations necessary to develop this model have been included in the Appendix.

Nomenclature

A_m'	=	A_m/t_c', frequency factor in the devolatilization rate expression (Eq. 38), 1/sec
B_k	=	Transfer Number (see Eq. 31)
C_D	=	drag coefficient
C_p'	=	C_p C_{pg}', gas-phase specific heat, Cal/gm/ok
C_{pk}'	=	C_{pk} C_{pg}', condensed-phase specific heat
C_{pc}'	=	C_{pc} C_{pg}', coal specific heat
C_{pw}'	=	C_{pw} C_{pg}', water specific heat
D'	=	D D_g', gas-phase diffusion coefficient, cm^2/sec
D_g'	=	Reference value of the diffusion coefficient
d_s'	=	droplet spacing, cm
E_m'	=	T_m T_β' R', activation energy in the devolatilization reaction rate (Eq. 38) Cal/mole
H_k'	=	H_k $C_{pg}'T_g'$, heat given to the particle from the gas-phase during water vaporization, Cal/gm

I_w = parameter to distinguish between the water vaporization and devolatilization

K_m' = K_m / t_g', in the devolatilization reaction rate term (see Eq. 37)

L_g' = Tube length, also the gas-phase characteristic length, cm

L_r = L_g' / r_{ko}'

L_w' = $L_w C_{pg}' T_g'$, Heat of vaporization for water, Cal/gm

M_a' = Molecular weight of air, gm/mole

M_w' = Molecular weight of water

m_k' = $m_k r_{ko}^{3\prime} \rho_{kc}'$, particle mass, gm

m_{chk}' = $m_{chk} r_{ko}^{3\prime} \rho_{kc}'$, char mass in one particle, gm

m_{rk}' = $m_{rk} r_{ko}^{3\prime} \rho_{kc}'$, raw coal mass in one particle

m_{ak}' = $m_{ak} r_{ko}^{3\prime} \rho_{kc}'$, ash mass in one particle

M_{wk}' = $M_{wk} (t_r L_g' \rho_g' / t_g' L_r)$, water vaporization rate, gm/sec

M_{vk}' = $M_{vk} \rho_g' L_g'^3 / t_g'$, devolatilization rate, gm/sec

n_k' = n_k / L_c', number of particles per unit cross sectional area of the tube, $1/cm^2$

p' = $p\, p_g'$, pressure, atm

p_n' = normal pressure (1 atm)

Q' = $Q C_{pg}' T_g' r_{ko}' \rho_g' D_g'$, heat given to the particle from the gas-phase after water vaporization

r_c' = $r_c\ r_{ko}'$, coal particle radius, cm

r_k' = $r_k\ r_{ko}'$, particle radius, cm

r_{ko}' = initial particle radius, cm

R' = gas constant, Cal/mole/°K

R_g' = gas constant, atm cm^3/mole/°K

R_{ek} = Reynolds number (see Eq. 21)

R_f = convective correction (see Eq. 32)

S = non-dimensional source term for the gas-phase

t' = $t\ t_g'$, time, sec

t_g' = L_g'/V_g'

t_r = $t_g'/(L_g'^2/D_g')$

T' = $T\ T_g'$, gas-phase temperature, °K

T_k' = $T_k\ T_g'$, particle temperature

T_{bn}' = boiling temperature of water at normal pressure (1 atm)

V' = $V\ V_g'$, gas-phase velocity, cm/sec

V_k' = $V_k\ V_g'$, particle velocity

X' = $X\ L_g'$, spatial coordinate, cm

X_k' = $X_k\ L_g'$, particle position, cm

X_{ws} = water vapor mole fraction at the particle surface

Y = mass fraction, also the variable used in Eq. (2)

Y_{ws} = water vapor mass fraction at the surface

a_m = mass stoichiometry coefficient (see Eq. 37)

$\Delta x'$ = $\Delta x\ L_g'$, spatial step size, cm

$\Delta t'$	=	$\Delta t\ t_g'$, temporal step size, sec
μ'	=	gas viscosity, gm/cm/sec
Φ	=	$\Phi\ T_g'\ (p_g'^{\gamma})$ transformed temperature (see Eq. 6)
γ	=	ratio of specific heats
ρ	=	$\rho\ \rho_g'$, gas-phase density, gm/cm^3
ρ_k'	=	$\rho_k\ \rho_{ko}'$, particle density
ρ_1	=	ρ_g'/ρ_{ko}'
ρ_c'	=	$\rho_c\ \rho_{kc}'$, coal density
ρ_w'	=	$\rho_w\ \rho_{kc}'$, water density

SUBSCRIPTS

a	-	air
c	-	coal
g	-	reference value used for non-dimensionalization
k	-	particle, also the particle group number
m	-	devolatilization reaction rate number
n	-	neutral species (Eq. 5)
o	-	initial value, also oxidizer
s	-	particle surface
v	-	volatile

w - water

SUPERSCRIPT

/ - dimensional variable

References

1. R. R. Solomon and M. B. Colket, Seventeenth Symposium (International) on Combustion 131, 1978.

2. E. M. Suuberg, W. A. Peters, and J. B. Howard, Seventeenth Symposium (International) on Combustion 117, 1978.

3. L. Douglas Smoot, Eighteenth Symposium (International) on Combustion 117, 1980.

4. Unger and Suuberg, Eighteenth Symposium (International) on Combustion 1203, 1980.

5. Aggarwal, S. K., Tong, A. Y., and Sirignano, W.A., "A Study of Inter-phase Exchange Laws in Spray Combustion Modeling," Paper No. A1AA-83-0152, 21st Aerospace Sciences Meeting, Reno, Nevada, Jan. 10-13, 1983.

6. Ranz, W. E. and Marshall, W. R., "Evaporation from Drops," Chemical Engineering Progress, Vol. 48, pp. 141-146 and 173-180, 1952.

7. Ubhayakar, S. K. Stickler, D. B., Von Rosenberb, Jr., C. W., and Gannon, R. E., "Rapid Devolatilization of Pulverized Coal in Hot Combustion Gases," Sixteenth Symposium (International) on Combustion, The Combustion Institute, pp. 427-436, 1976.

8. Kobayashi, H., Howard, J. B., and Sarofim, A. F., "Coal Devolatilization at High Temperatures," Sixteenth Symposium (International) on Combustion, The Combustion Institute, pp. 411-425, 1976.

9. Smith, P. J. and Smoot, L. D., "One-Dimensional Model for Pulverized Coal Combustion and Gasification," Com. Sci. and Technol., Vol. 23, pp. 17-31, 1980.

Table 1

Values of Various Parameters Used in the Calculations

A_1'	=	3.75×10^5 1/sec
A_2'	=	1.46×10^{13} 1/sec
C_{pg}'	=	0.25 Cal/gm/°K
C_{pw}'	=	1.0 Cal/gm/°K
C_{pc}'	=	0.3 Cal/gm/°K
d_s'	=	0.05 cm
E_1'	=	17600 Cal/mole
E_2'	=	60000 Cal/mole
L_g'	=	10 cm
L_w'	=	480 Cal/mole
M_a'	=	28.0 mole/gm
M_w'	=	18.0 mole/gm
n_k'	=	400 $1/cm^2$
p_g'	=	10 atm.
R'	=	1.98717 Cal/mole/°K
R_g'	=	2.05576 atm cm^3/mole/°K
r_{ko}'	=	50 μm
r_{co}'	=	initial coal particle radius = $(.5)^{1/3}\ r_{ko}'$

$T_{bn}' = 373°K$

$T_{ko}' = 300°K$

$T_g' = 1500°K$

$V_g' = 200$ cm/sec

$\alpha_1 = 0.39$

$\alpha_2 = 0.80$

$\Delta x' = 0.1$ cm

$\Delta t' = 10^{-5}$ sec

$\gamma = 1.38$

$\mu_g' = 5.2597 \times 10^{-4}$ gm/cm/sec

$\rho_g' = 2.3488$ gm/cm^3

$\rho_w' = 0.99$ gm/cm^3

$\rho_c' = 1.485$ gm/cm^3

APPENDIX

Approach to Scaling of Devolatilization Rates

Consider a volatile species forming as a gas in the interior of the coal. Assume spherical symmetry. The radial velocity

$$u(r) = - k \frac{\partial p}{\partial r}$$

where p is the pressure and k has units of length divided by the product of density and velocity or equivalently length squared divided by kinematic viscosity. Since we expect that the flow has a very low Reynolds number on account of the fine pore structure, a friction-dominated flow is expected.

For the moment, we can assume that the pressure of the trapped volatile gas in the pores is proportional to the product of a gas density and the temperature. The gas temperature and the solid (or liquid) temperature will be assumed to be identical for a given neighborhood in the coal particle. So $p = \rho_g RT$.

There is some question about this assumption if the pore size is as small as the average distance between molecules of the gas. Let us assume that is not the case.

Furthermore, we shall consider a uniform but time-varying temperature through the particle. Then

$$u = - k \frac{\partial p}{\partial r} = - k\, RT \frac{\partial \rho_g}{\partial r}$$

Here k is given by a characteristic length (pore size) squared divided by an effective viscosity. This viscosity should be proportional to gas density times a speed of sound times a characteristic length. It follows that

$$k = \ell^2 / \mu_{eff} \sim \frac{\ell^2}{\rho_g\, c_g\, \ell} \sim \frac{\ell}{\rho_g\, R^{1/2}\, T^{1/2}}$$

so that

$$u = - \text{constant.} \quad \frac{\ell\ RT}{\rho_g} \frac{\partial \rho_g}{\partial r}$$

The above assumes that a molecular mean free path is longer than the pore size. Perhaps this condition is violated at very high pressures.

Consider now a conservation equation for the volatile species in the coal

$$r^2 \frac{\partial (\rho_g \epsilon)}{\partial t} + \frac{\partial}{\partial r} \left(\tilde{\epsilon}\ \rho_g\, u r^2 \right) = r^2\, S_v$$

$$r^2 \frac{\partial (\rho_g \epsilon)}{\partial t} = \text{constant,}\ R^{1/2}\, T^{1/2} \frac{\partial}{\partial r} \left(r^2 \tilde{\epsilon}\ \ell \frac{\partial \rho_g}{\partial r} \right) + r^2\, S_v$$

It can be shown that

$$\tilde{\epsilon} = n^{2/3} \frac{\pi}{4} \ell^2 \; ; \quad \epsilon = \frac{\pi}{6} n \ell^3$$

n = number density of pores; $s = n^{-1/3}$ = spacing between pores

$$\frac{\epsilon \ell}{\epsilon} = \frac{3}{2} n^{-1/3} = \frac{3}{2} s$$

Consider now that ϵ and $\tilde{\epsilon}$ change slightly with r and t

$$r^2 \frac{\partial \rho_g}{\partial t} = \text{constant } s \, T^{1/2} R^{1/2} \frac{\partial}{\partial r} \left(r^2 \frac{\partial \rho_g}{\partial r} \right) + r^2 \frac{S_v}{\epsilon}$$

It follows that $s \, T^{1/2} R^{1/2}$ is an effective diffusivity. If $s < \lambda$ the mean free path, then diffusion is slower in the particle than in the gas; if $s > \lambda$, faster diffusion occurs in the particle than in the gas. Note in either case, it is assumed that $\ell < \lambda$.

Note that if ℓ were greater than λ, it can be shown that the effective diffusivity would be ℓ/λ greater than shown.

If s is not too much smaller than λ the diffusion rate through the pores will not be too much less than the gas-phase diffusion rate. In that case, species diffusion through the pores might be just as rapid as heat diffusion through the solid material. In that case, one might assume a uniform but time-varying gas density in the pores as was done for the temperature. Then

$$\frac{d\rho_g}{dt} = \frac{S_v}{\epsilon}$$

The interesting finding is that this conclusion will hold for large s even if ℓ is very small. There is question though whether s and ℓ will be different in order of magnitude. Probably, it is reasonable to assume that they are the same order of magnitude and for not-too-high pressures, they will be smaller than a mean free path.

Let us examine the quantity S_v/ϵ. We expect that S_v (the mass of volatiles created per unit time per unit volume of the coal particle) is a function of the temperature, the hydrocarbon composition of the coal, and the surface area per unit volume in the pores. That is, $S_v \sim n\,\ell^2\,f$ (T, composition). It follows that

$$\frac{S_v}{\epsilon} = \frac{1}{\ell} f\ (T,\ \text{composition}) = \frac{f}{\ell}$$

For the simple model

$$\frac{d\rho_g}{dt} = \frac{f}{\ell}$$

and

$$\frac{d(\epsilon\rho_g)}{dt} = \frac{\epsilon f}{\ell} \sim n\,\ell^2\,f = \frac{\ell^2}{s^3} f$$

If $\ell = 0(s)$, then $\epsilon = 0(1)$ and

$$\frac{d(\epsilon\rho_g)}{dt} = 0\left(\frac{d\rho_g}{dt}\right) = 0\left(\frac{f}{\ell}\right) = 0\left(f\,n^{1/3}\right)$$

$\epsilon \rho_g$ is the mass of volatiles per unit volume of coal particle.

In this limit, the rate at which volatile mass is being created would equal

$$\frac{dM_v}{dt} = \int_0^R 4\pi r^2 \frac{\partial(\rho_g \epsilon)}{\partial t}\, dr = \frac{4\pi}{3} R^3 \frac{d(\epsilon \rho_g)}{dt}$$
$$= 0 \left(R^3 \; f \; n^{1/3}\right)$$

This would show a linear dependence upon the volume of the particle.

Let us now look at a model where mass diffusion in the particle is not so rapid compared to diffusion of heat. So temperature is uniform but time-varying while volatile density varies spatially and temporally through the particle.

Define a_v = constant s $T^{1/2} R^{1/2}$

$$r^2 \frac{\partial \rho_g}{\partial t} = a_v \frac{\partial}{\partial r}\left(r^2 \frac{\partial \rho_g}{\partial r}\right) + r^2 \frac{S_v}{\epsilon}$$

$$r^2 \frac{\partial \rho_g}{\partial t} = a_v \frac{\partial}{\partial r}\left(r^2 \frac{\partial \rho_g}{\partial r}\right) + r^2 \frac{f}{\ell}$$

Nondimensionalize

$$\eta = r/R , \qquad \tau = \frac{t a_v}{R^2} = \frac{t}{t_{diff}}$$

$$\theta = \rho_g / \rho_{ref} , \qquad \lambda = f/f_{ref}$$

$$t_{diff} = R^2/a_v , \qquad t_{chem} = (\delta_{ref}/\rho_{ref}\, \ell)^{-1}, \; D = \frac{t_{diff}}{t_{chem}}$$

$$\eta^2 \frac{\partial \theta}{\partial \tau} = \frac{\partial}{\partial \eta}\left(\eta^2 \frac{\partial \theta}{\partial \eta}\right) + \frac{R_2}{\ell a_v} \lambda \, \eta^2 \frac{f_{ref}}{\rho_{ref}}$$

$$\eta^2 \frac{\partial \theta}{\partial \tau} = \frac{\partial}{\partial \eta}\left(\eta^2 \frac{\partial \theta}{\partial \eta}\right) + D \, \lambda \, \eta^2$$

D is a damkohler number, also related to a Thiele modulus. For very small D, chemistry is rate-controlling and gradient disappear. This is the same case as before. For large D (compared to unity) diffusion is controlling and we may find a quasi-steady solution. This solution establishes itself after a characteristic diffusion time during which a transient occurs. It is assumed that the lifetime is long compared to the diffusion time.

The governing equation becomes

$$\frac{\partial}{\partial \eta}\left(\eta^2 \frac{\partial \theta}{\partial \eta}\right) = - D \, \lambda \, \eta^2$$

$$\text{At} \quad \eta = 0 , \quad \frac{\partial \theta}{\partial \eta} = 0$$

Integrating, we have

$$\eta^2 \frac{\partial \theta}{\partial \eta} = - D \int_0^{\eta} \lambda \, (\eta'^1)^2 \, d\eta'$$

or at $\eta = 1$

$$\frac{\partial \theta}{\partial \eta} = - D \int_o^1 \lambda \, \eta^2 \, d\eta$$

Now, mass flux from surface is given by

$$\frac{dM_v}{dt} = 4 \pi \rho_g \, n \, R^2 \, \tilde{\epsilon} = 4 \pi \, \tilde{\epsilon} \, R^2 \left(- \text{constant } \ell \quad RT \quad \frac{\partial \rho_g}{\partial r} \right)$$

$$= 4 \pi \, \tilde{\epsilon} \, R^2 \, \ell \quad RT \quad \frac{\rho_{ref}}{R} \left(- \text{constant} \frac{\partial \theta}{\partial \eta} \right)$$

$$= 4 \pi \, \tilde{\epsilon} \, \ell \quad RT \, \rho_{ref} \, (\text{constant}) \, R \, D \int_o^1 \lambda \, \eta^2 \, d\eta$$

Since $D \sim R^2$ we have

$$\frac{dM_v}{dt} \sim R^3.$$

So again we can expect a devolatilization rate proportional to R^3. Further

$$\tilde{\epsilon} \, \ell \quad RT \quad \rho_{ref} \, R \, D = \tilde{\epsilon} \, \ell \quad RT \quad \rho_{ref} \, R \, \frac{R^2}{a_v} \left(\frac{\rho_{ref} \, \ell}{f_{ref}} \right)^{-1}$$

$$= n^{2/3} \, \frac{\pi}{4} \, \ell^3 \quad RT \quad \frac{f_{ref}}{\ell} \quad R^3 \quad \frac{1}{\text{constant.s.} \quad RT}$$

$$= 0\left(\frac{f_{ref}}{\ell s}\ \ell^3\ n^{2/3}\ R^3\right)$$

Now if $s = 0(\ell) = 0\ (n^{-1/3})$, the above is of order of

$$\frac{f_{ref}}{\ell} R^3 = 0\left(f_{ref}\ R^3\ n^{+1/3}\right)$$

Basically, this is the same result as before.

Examine the transient behavior leading to this quasi-steady asymptotic. We could solve partial differential equations but first we model as

$$\frac{d\rho_g}{dt} = -\frac{\alpha_v}{R^2}\rho g + \frac{f}{\ell}$$

or

$$\frac{d\theta}{d\tau} = -\theta + \lambda D$$

$$\frac{\theta-\lambda D}{\theta_o-\lambda D} = e^{-\tau}$$

$$\theta_o = 0$$

$$\theta = \lambda D\left(1 - e^{-\tau}\right)$$

$$\rho_g = \lambda D\ \rho_{ref}\left(1 - e^{-t\ \alpha_v/R^2}\right)$$

The amount diffused to the outside is

$$\frac{dM_v}{dt} = \frac{4\pi}{3} R^3 \epsilon \rho_g \frac{a_v}{R^2} = \frac{4\pi}{3} \epsilon R a_v \rho_g$$

$$\frac{dM_v}{dt} = \frac{4\pi}{3} \epsilon a_v \lambda \rho_{ref} D R \left(1 - e^{-t a_v/R^2}\right)$$

$$\frac{dM_v}{dt} = \frac{4\pi}{3} \epsilon \lambda \frac{f_{ref}}{\ell} \left(1 - e^{-t a_v/R^2}\right)$$

Note

$$\frac{4\pi}{3} \Sigma \lambda \frac{f_{ref}}{\ell} R^3 = 0\left(\frac{f_{ref}}{\ell} R^3\right)$$

Again we see asymptotically the same order of magnitude with a transient time of the order of the diffusion time

For $t \ll R^2/a_v$, it follows that

$$1 - e^{-t a_v/R^2} \approx a_v t/R^2$$

and

$$\frac{dM_v}{dt} = 0\left(\frac{f_{ref}}{\ell} R a_v t\right)$$

while for $t \gg R^2/a_v$

$$\frac{dM_v}{dt} = 0\left(\frac{f_{ref}}{\ell} R^3\right)$$

So with time the sealing with R will change significantly. If the devolatilization time is not greater than the diffusion time (a possibility at very high temperatures), the R^3 dependence will not be reached.

The governing equations become more complicated when we account for: (i) spatial variations in temperature, and (ii) temporal and spatial variations in composition which affect the devolatilization rate.

The ideas proposed in the above section are refinements that must be incorporated in any future modeling effort. It is expected that a better fit with experimental data would be obtained based on the proposed model.

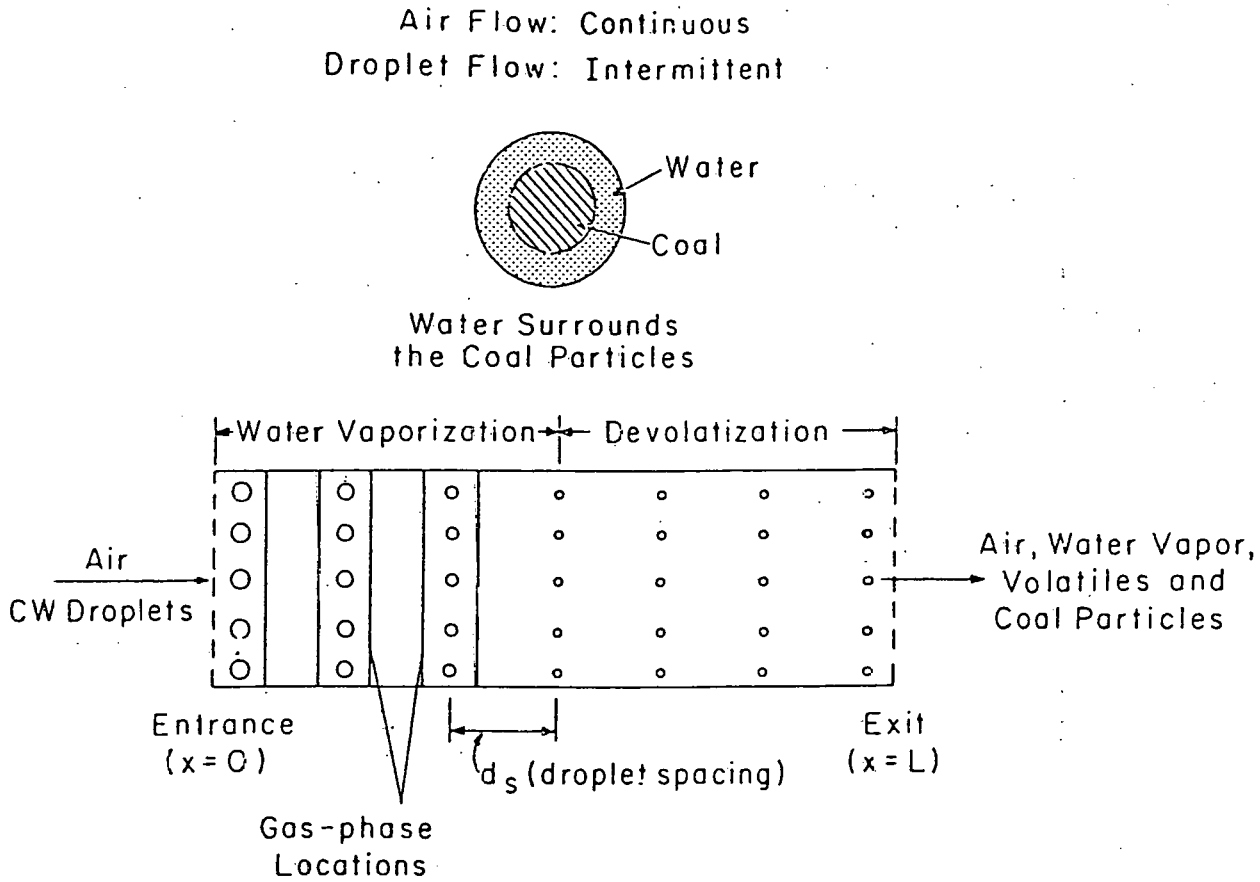

Fig. 1. Schematic of Physical Model

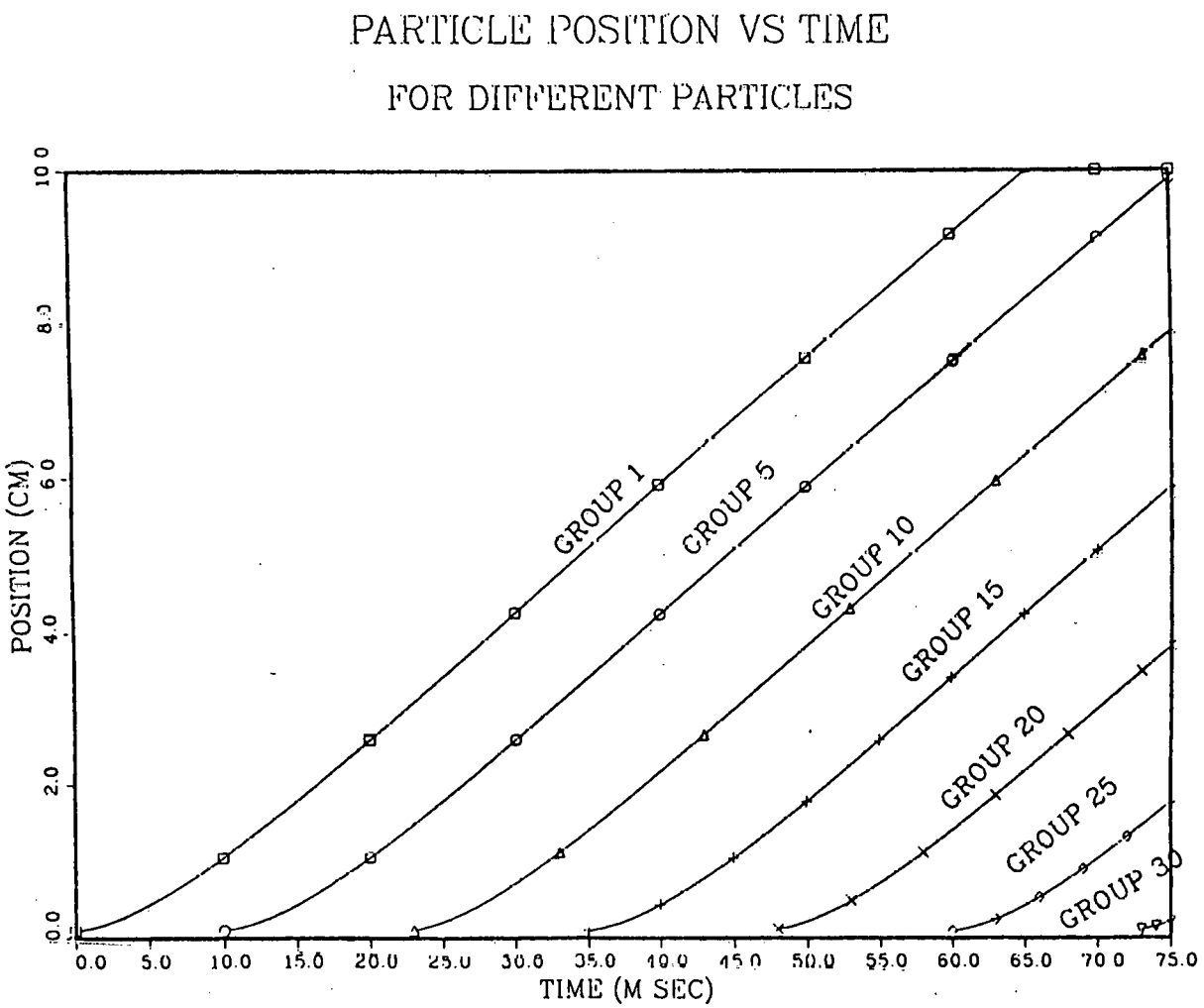
PARTICLE POSITION VS TIME
FOR DIFFERENT PARTICLES
POSITION (CM)
0.0
2.0
4.0
6.0
8.0
10.0
0.0
5.0
10.0
15.0
20.0
25.0
30.0
35.0
40.0
45.0
50.0
55.0
60.0
65.0
70.0
75.0
TIME (M SEC)
GROUP 1
GROUP 5
GROUP 10
GROUP 15
GROUP 20
GROUP 25
GROUP 30

FIGURE 2

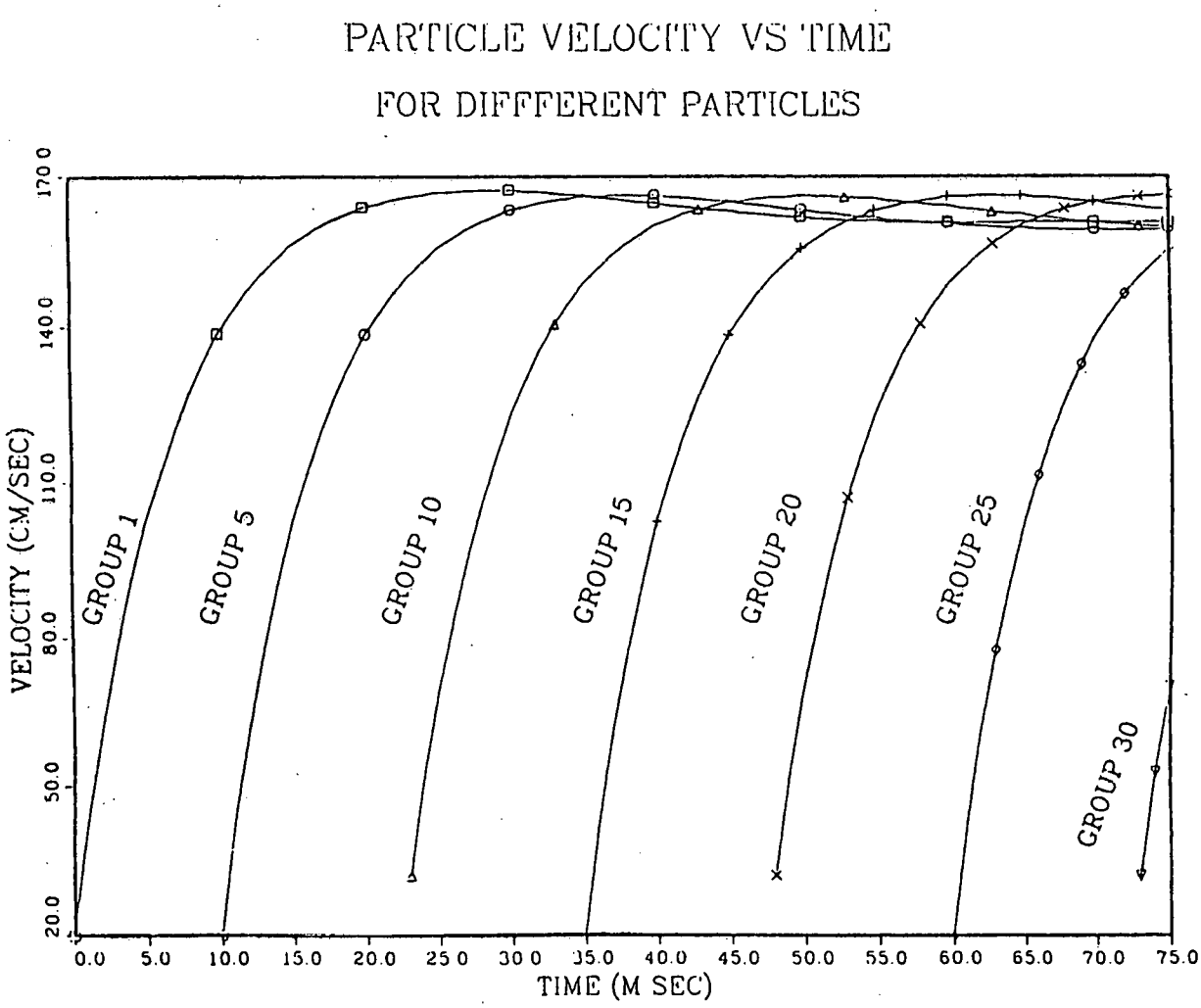
PARTICLE VELOCITY VS TIME
FOR DIFFFERENT PARTICLES
VELOCITY (CM/SEC)
170.0
140.0
110.0
80.0
50.0
20.0
GROUP 1
GROUP 5
GROUP 10
GROUP 15
GROUP 20
GROUP 25
GROUP 30
0.0
5.0
10.0
15.0
20.0
25.0
30.0
35.0
40.0
45.0
50.0
55.0
60.0
65.0
70.0
75.0
TIME (M SEC)

FIGURE 3

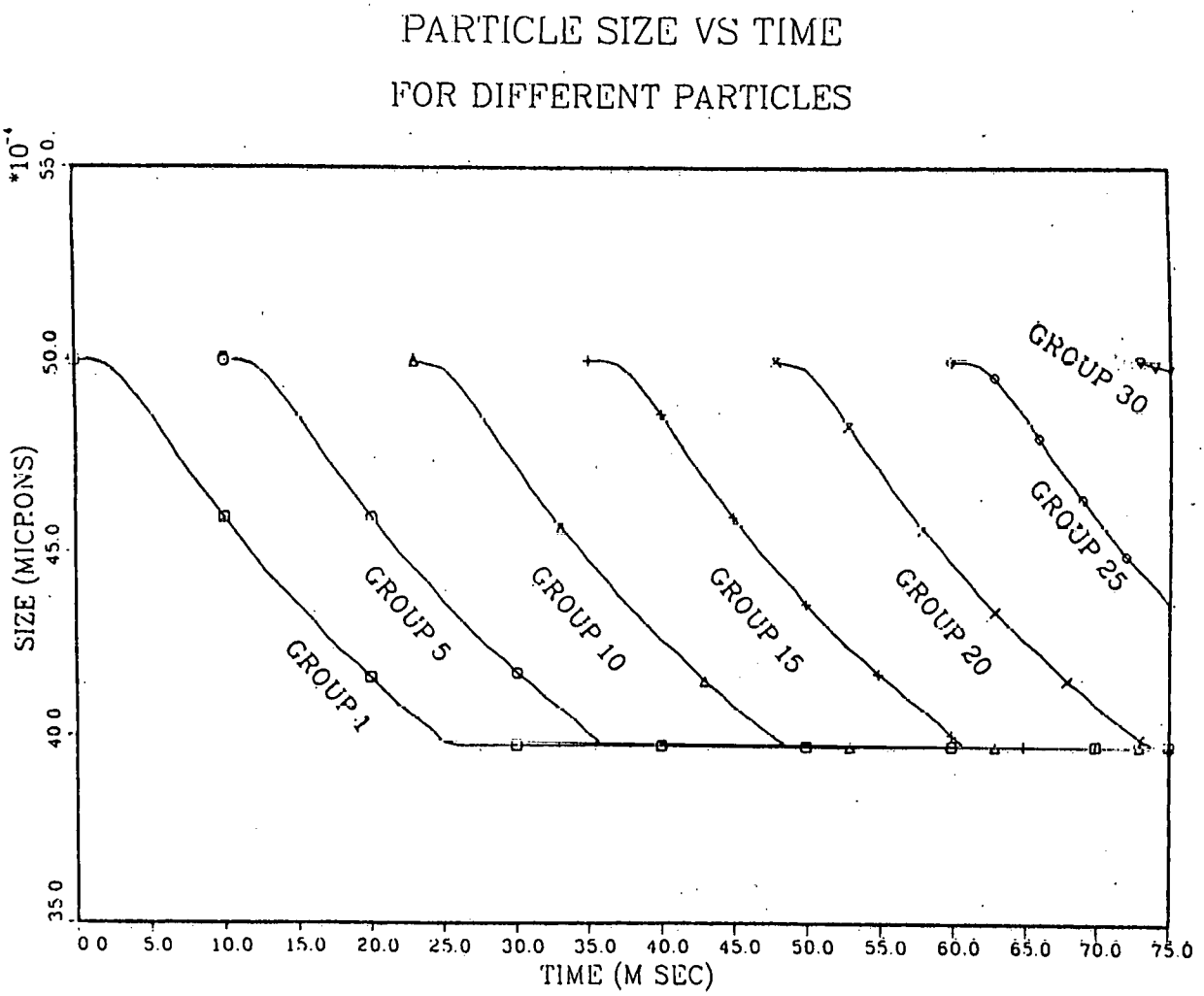
PARTICLE SIZE VS TIME
FOR DIFFERENT PARTICLES
*10⁻⁴
55.0
50.0
45.0
40.0
35.0
SIZE (MICRONS)
GROUP 1
GROUP 5
GROUP 10
GROUP 15
GROUP 20
GROUP 25
GROUP 30
0.0
5.0
10.0
15.0
20.0
25.0
30.0
35.0
40.0
45.0
50.0
55.0
60.0
65.0
70.0
75.0
TIME (M SEC)

FIGURE 4

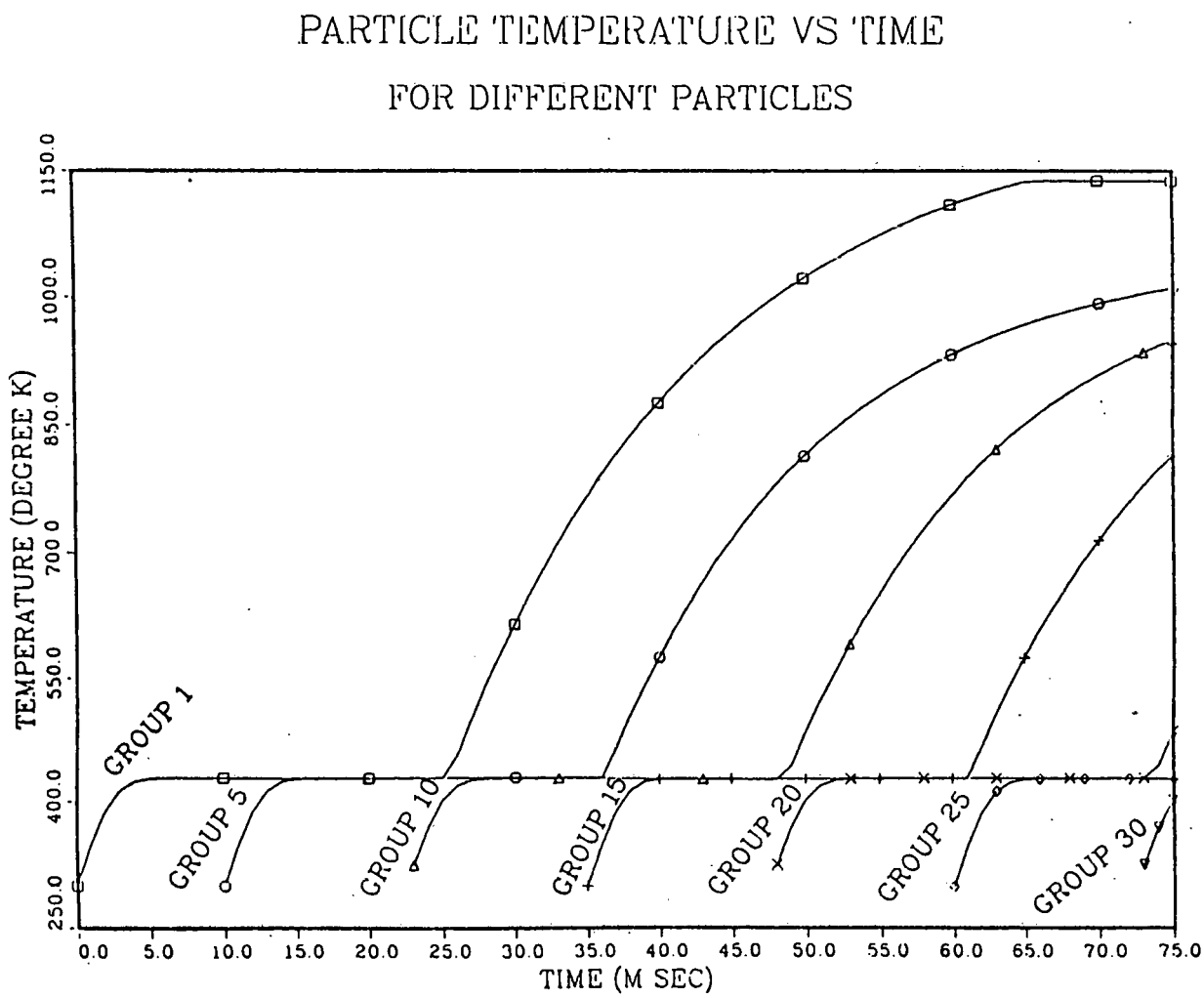
PARTICLE TEMPERATURE VS TIME
FOR DIFFERENT PARTICLES
TEMPERATURE (DEGREE K)
250.0
400.0
550.0
700.0
850.0
1000.0
1150.0
TIME (M SEC)
0.0
5.0
10.0
15.0
20.0
25.0
30.0
35.0
40.0
45.0
50.0
55.0
60.0
65.0
70.0
75.0
GROUP 1
GROUP 5
GROUP 10
GROUP 15
GROUP 20
GROUP 25
GROUP 30

FIGURE 5

PARTICLE DENSITY VS TIME

FOR DIFFFERENT PARTICLES

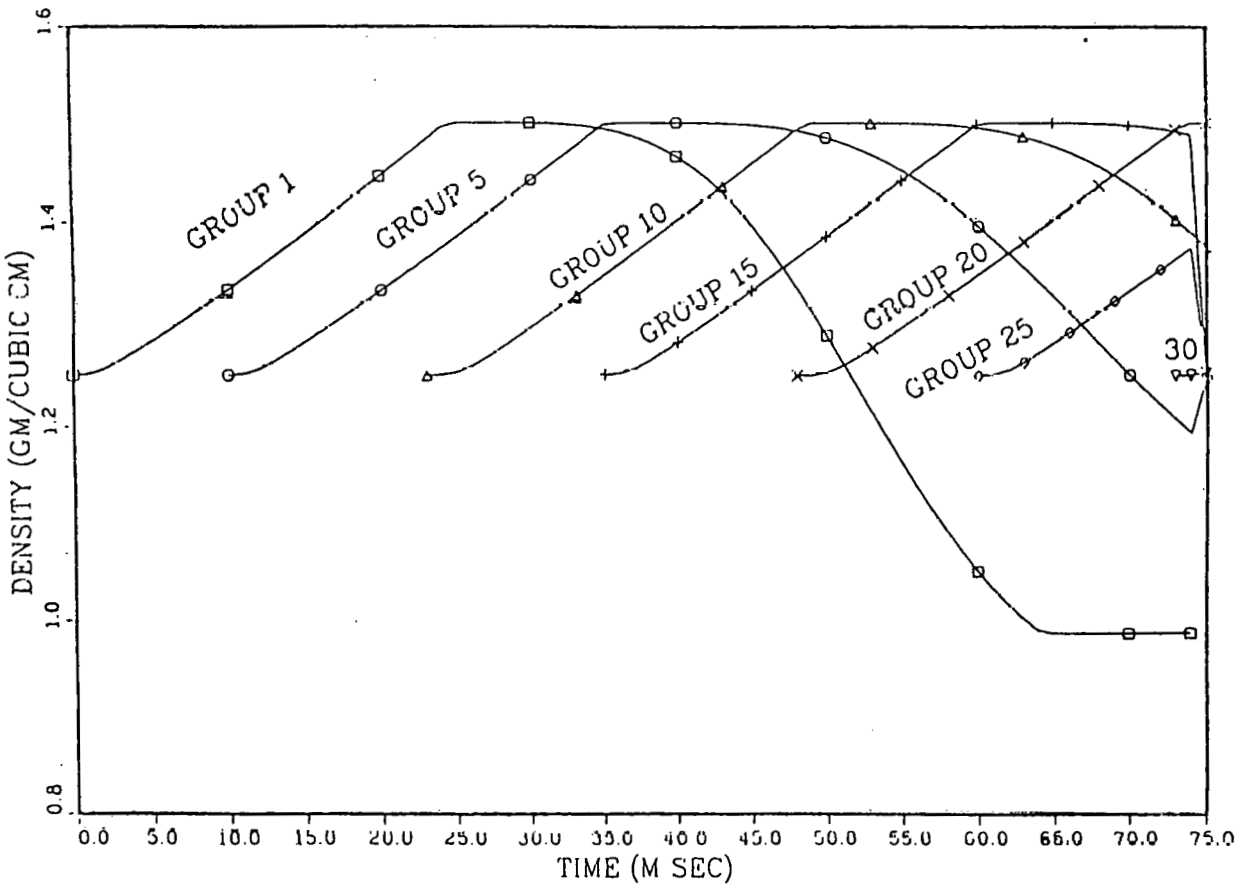

FIGURE 6

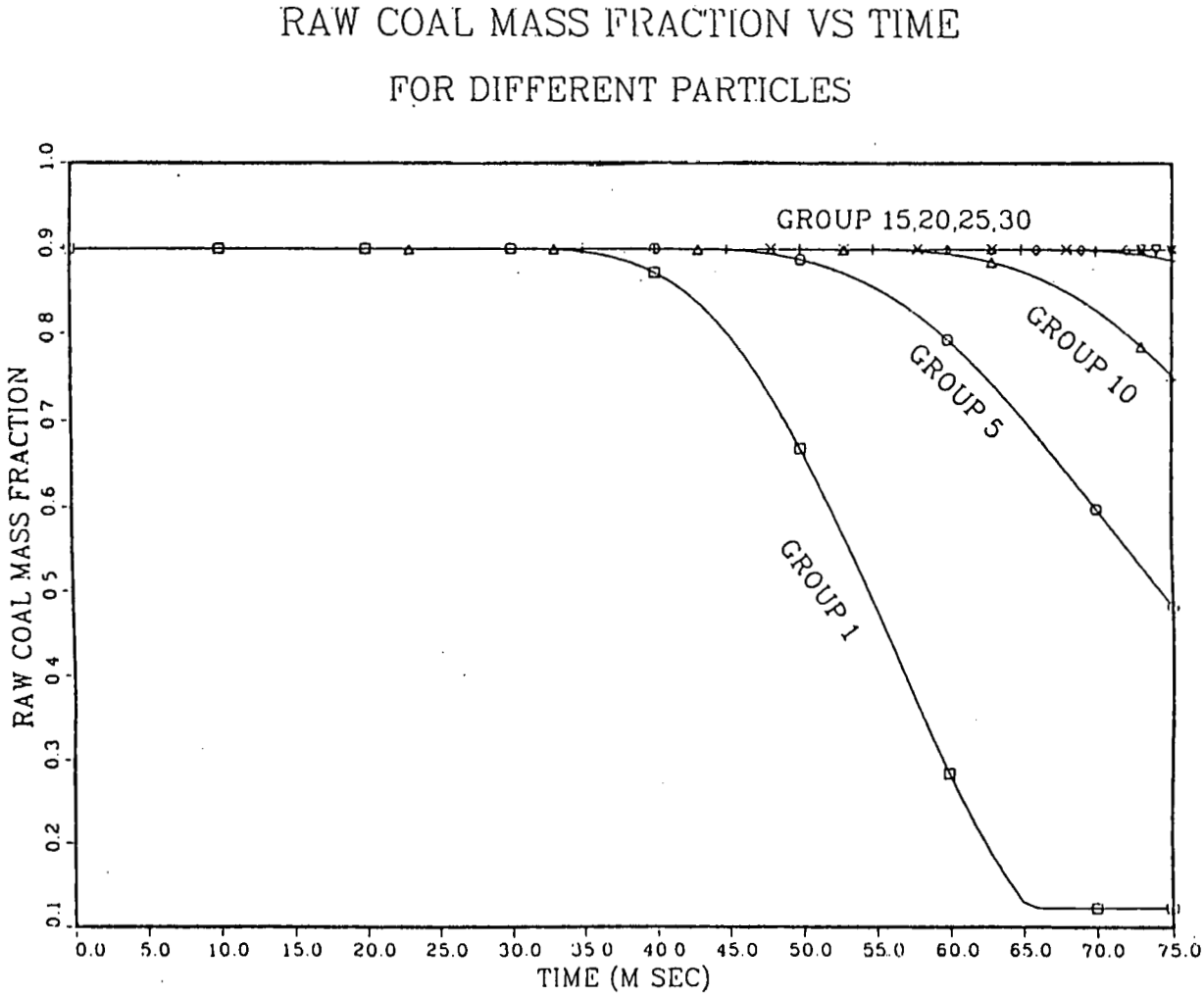
RAW COAL MASS FRACTION VS TIME
FOR DIFFERENT PARTICLES
GROUP 15,20,25,30
GROUP 10
GROUP 5
GROUP 1
RAW COAL MASS FRACTION
TIME (M SEC)
0.1
0.2
0.3
0.4
0.5
0.6
0.7
0.8
0.9
1.0
0.0
5.0
10.0
15.0
20.0
25.0
30.0
35.0
40.0
45.0
50.0
55.0
60.0
65.0
70.0
75.0

FIGURE 7

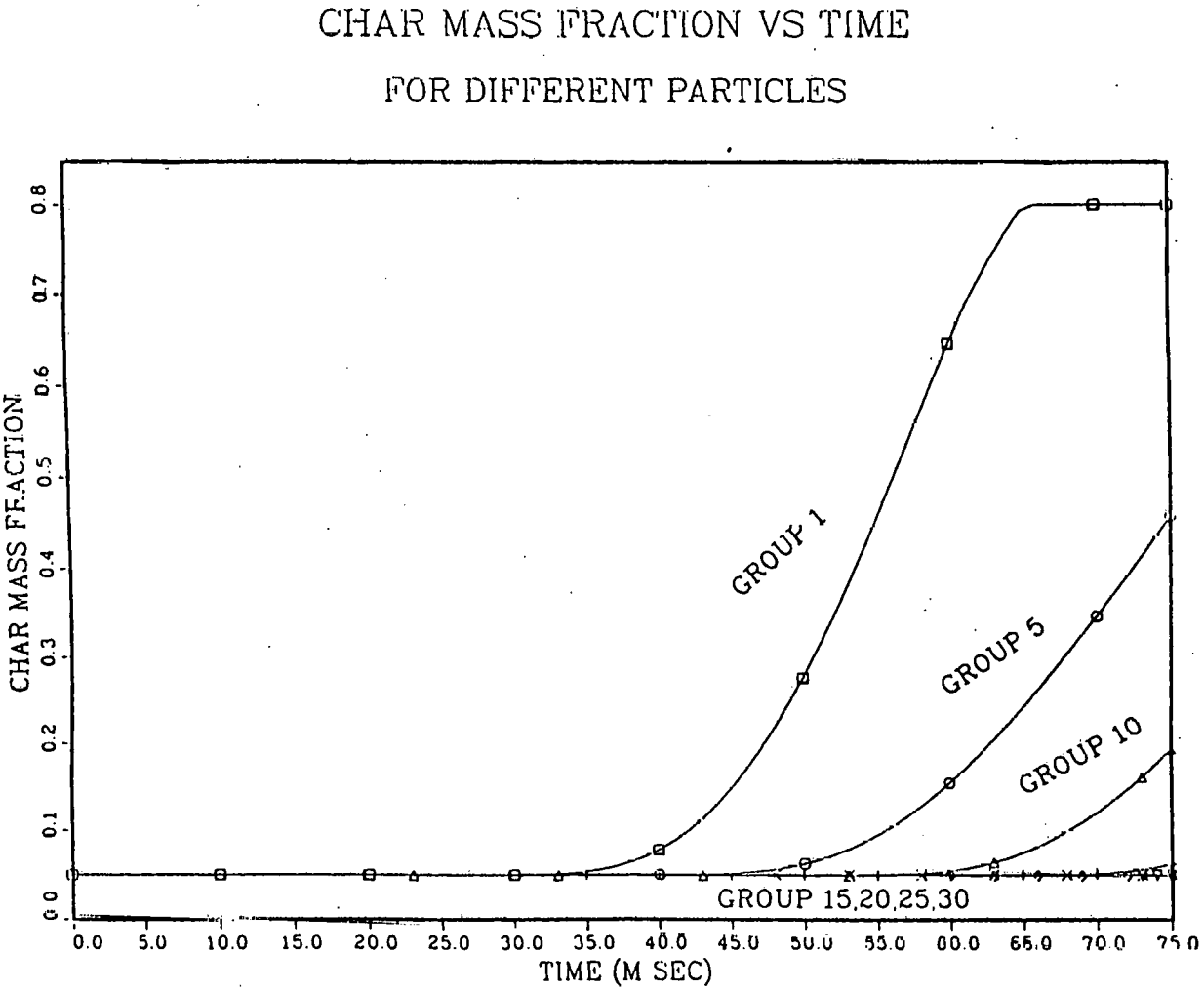
CHAR MASS FRACTION VS TIME
FOR DIFFERENT PARTICLES
CHAR MASS FRACTION
0.0
0.1
0.2
0.3
0.4
0.5
0.6
0.7
0.8
GROUP 1
GROUP 5
GROUP 10
GROUP 15,20,25,30
0.0 5.0 10.0 15.0 20.0 25.0 30.0 35.0 40.0 45.0 50.0 55.0 60.0 65.0 70.0 75.0
TIME (M SEC)

FIGURE 8

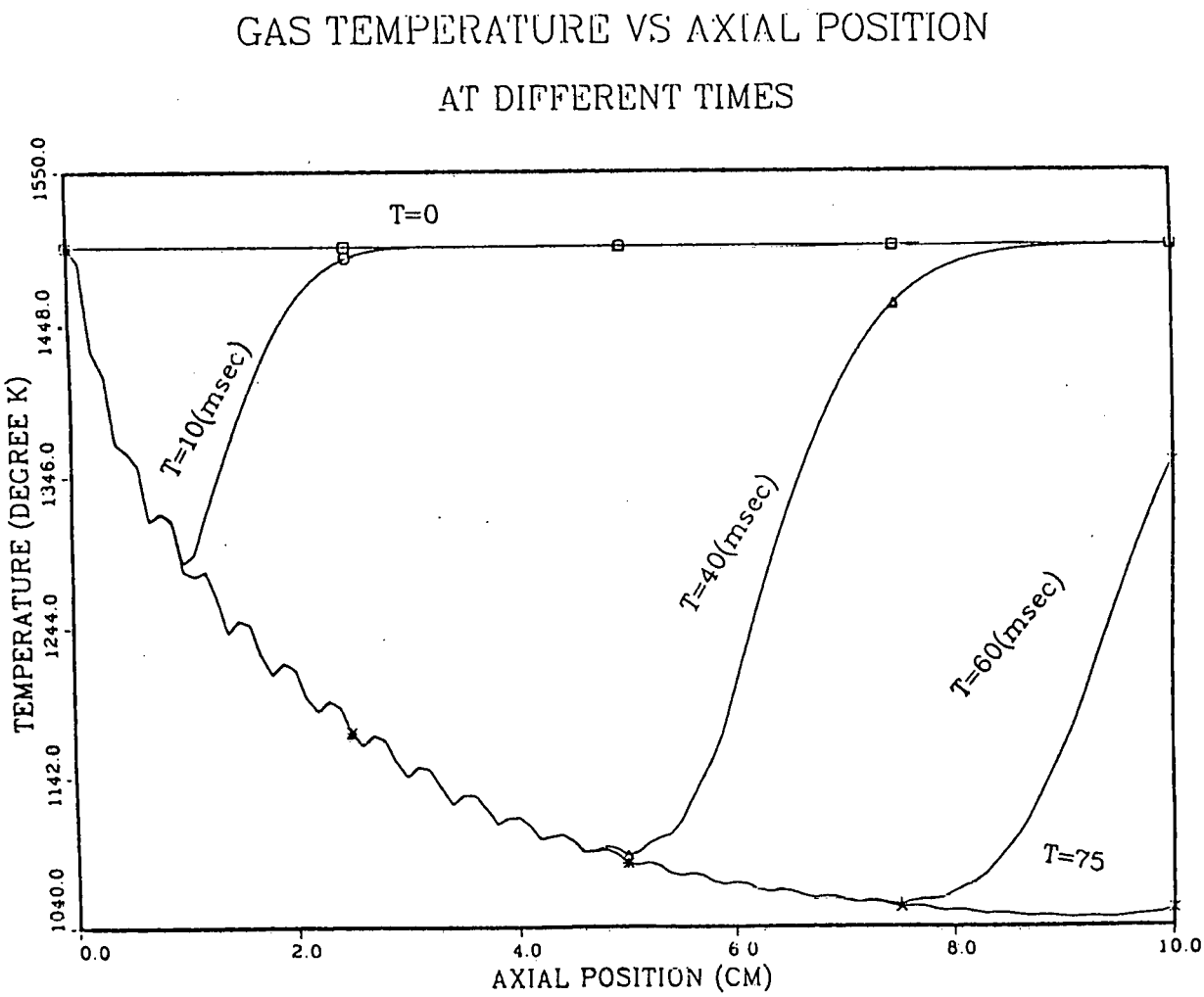
GAS TEMPERATURE VS AXIAL POSITION
AT DIFFERENT TIMES
TEMPERATURE (DEGREE K)
1550.0
1448.0
1346.0
1244.0
1142.0
1040.0
T=0
T=10(msec)
T=40(msec)
T=60(msec)
T=75
0.0
2.0
4.0
6.0
8.0
10.0
AXIAL POSITION (CM)

FIGURE 9

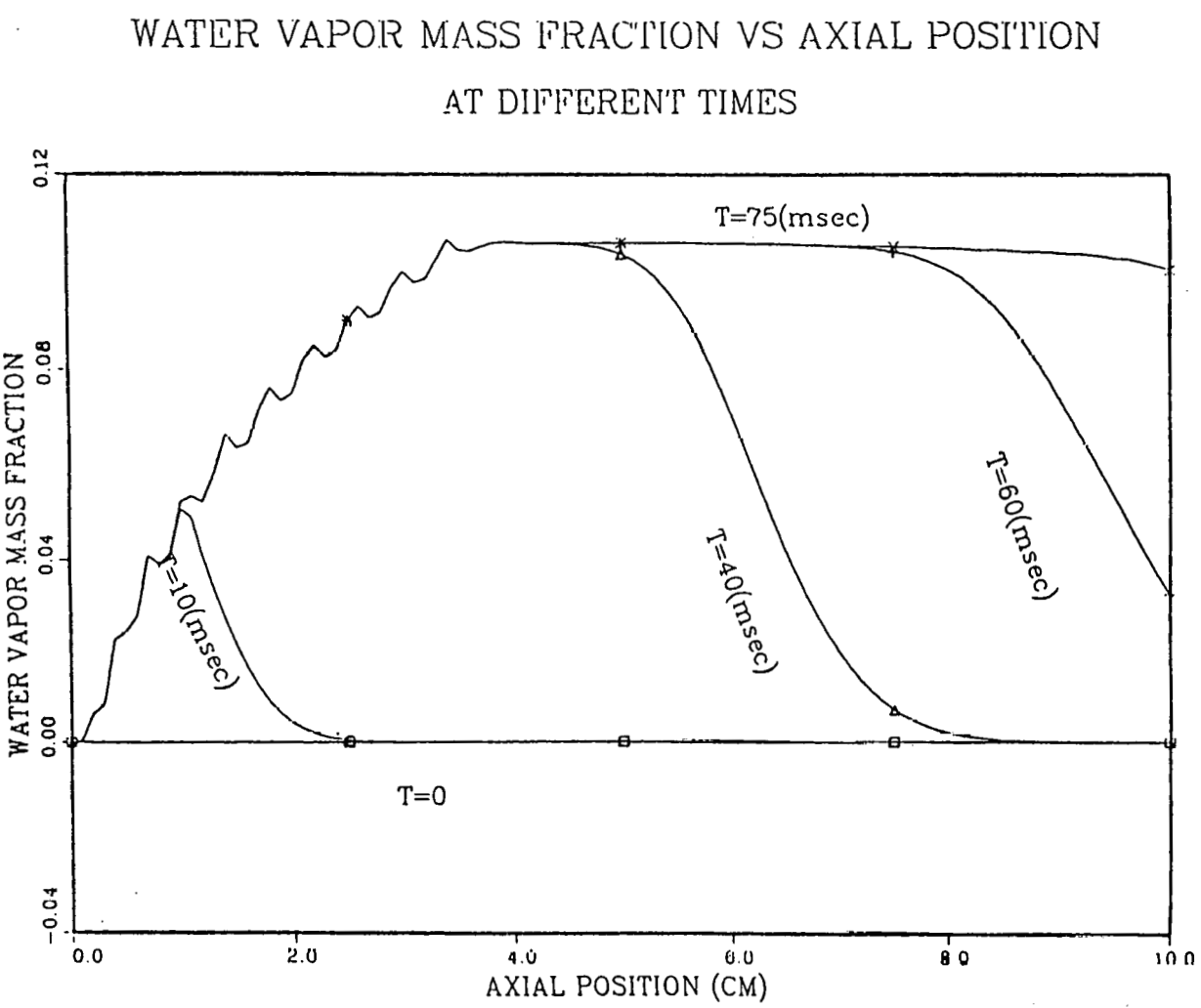
WATER VAPOR MASS FRACTION VS AXIAL POSITION
AT DIFFERENT TIMES
WATER VAPOR MASS FRACTION
0.12
0.08
0.04
0.00
-0.04
T=75(msec)
T=10(msec)
T=40(msec)
T=60(msec)
T=0
0.0
2.0
4.0
6.0
8.0
10.0
AXIAL POSITION (CM)

FIGURE 10

GAS VOLATILES MASS FRACTION VS AXIAL POSITION

AT DIFFERENT TIMES

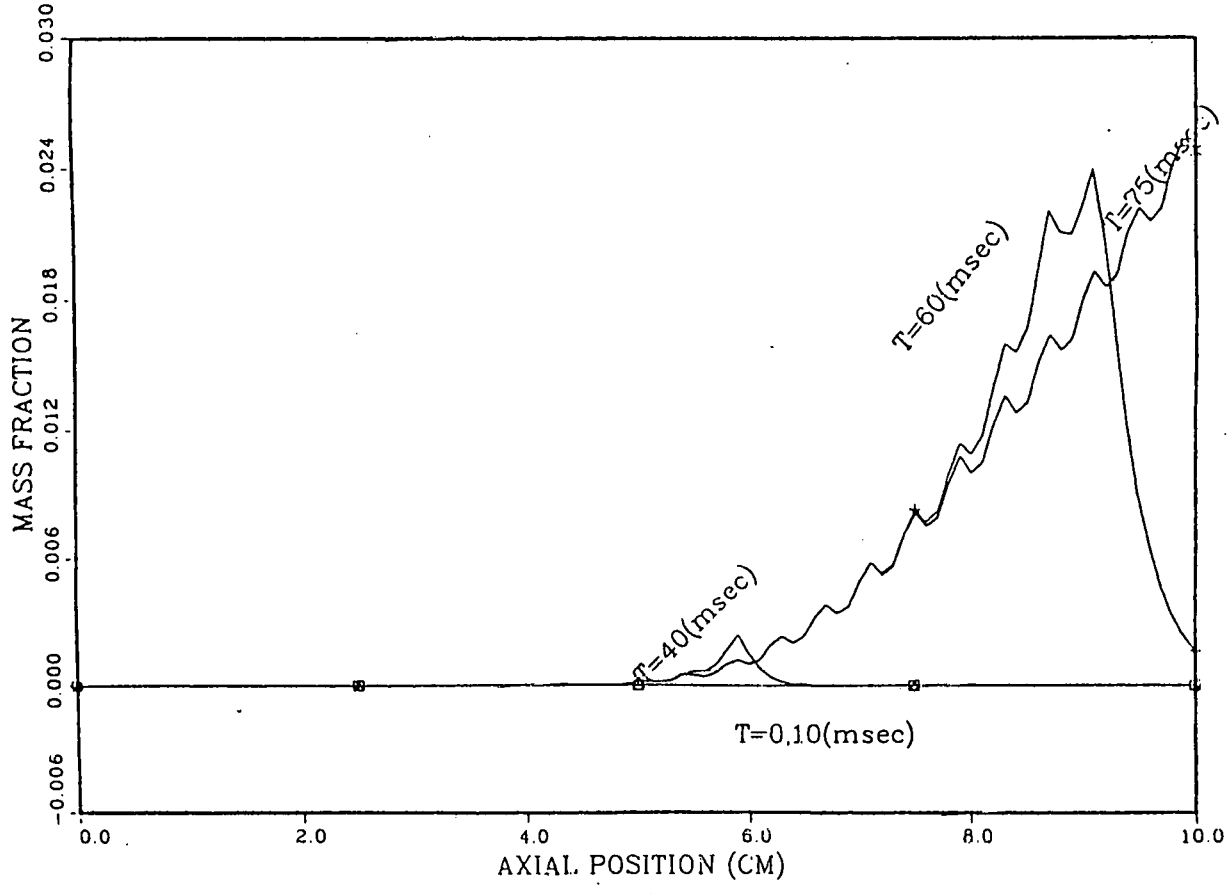

FIGURE 11

GAS VELOCITY VS AXIAL POSITION

AT DIFFERENT TIMES

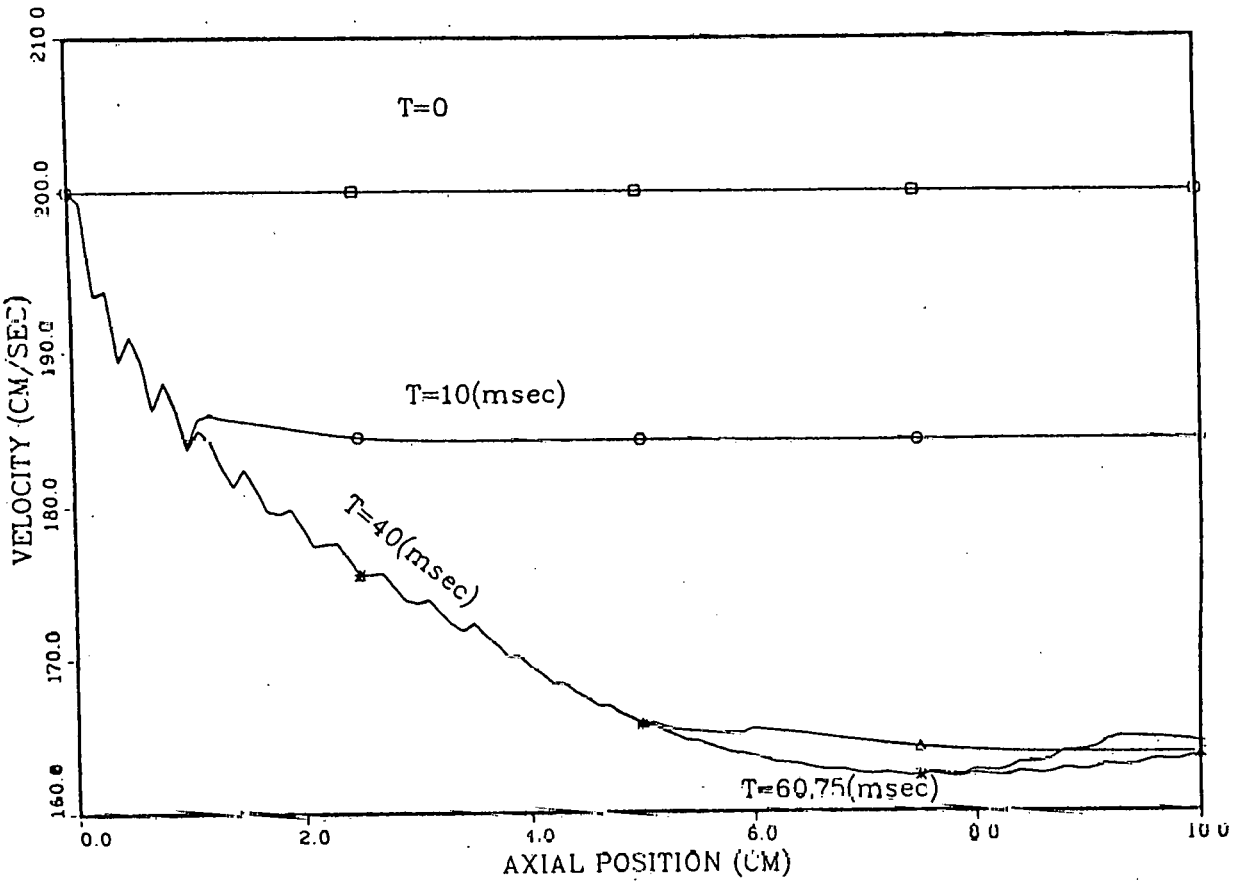

FIGURE 12

☆ U.S. GOVERNMENT PRINTING OFFICE: 1984—746-081/2600